Application of the timedependent Hartree grid–configuration interaction method to the desorption of diatomic molecules from solid surfaces

José CamposMartínez and Rob D. Coalson

Citation: J. Chem. Phys. **99**, 9629 (1993); doi: 10.1063/1.465496

View online: http://dx.doi.org/10.1063/1.465496

View Table of Contents: http://jcp.aip.org/resource/1/JCPSA6/v99/i12

Published by the AIP Publishing LLC.

Application of the time-dependent Hartree grid–configuration interaction method to the desorption of diatomic molecules from solid surfaces

José Campos-Martínez[a] and Rob D. Coalson[b]
Department of Chemistry, University of Pittsburgh, Pittsburgh, Pennsylvania 15260

(Received 1 March 1993; accepted 12 July 1993)

We study UV laser induced photodesorption of diatomic molecules from solid surfaces by means of the time-dependent Hartree grid–configuration interaction (TDHG–CI) method [J. Chem. Phys. **93**, 4740 (1990)]. Converged partial and total absorption cross sections are computed in several cases to demonstrate the flexibility and accuracy of the method. Comparison to TDHG results without CI corrections is also made. The failure of simple TDHG dynamics to reproduce state resolved rotational cross sections in various strong coupling limits is noted as a justification for the development of TDHG–CI algorithms.

I. INTRODUCTION

In recent years time-dependent methods have emerged as very useful tools in the field of quantum molecular dynamics.[1] Central to this growth has been the development of new propagation techniques[2] as well as new approximate methods.[3] Among these, the time-dependent Hartree (TDH) approach[4] has become one of the most widely used[3] and tested.[5] While the time-independent counterparts of these quantum methods are well established, they usually cannot be applied to more than 3 degrees of freedom. When the desired eigenfunctions are expanded in an appropriate basis, the number of these basis states (or channels) becomes prohibitively high, since the number of basis states needed grows geometrically with the spatial dimensionality of the problem, and computational effort scales as the number of basis states cubed. Besides, in dealing with multidimensional or polyatomic problems, it is intuitively appealing to utilize a classical or semiclassical approach for most of the degrees of freedom, while the few for which *quantum effects* are most important are treated by some available quantum method.[6,7] Time-independent methods are not easy to combine with other classical or semiclassical approaches,[6,3(a)] and therefore are not very useful for treating polyatomic molecules or condensed phase aggregates.

Time-dependent methods are more flexible in this regard. Since standard exact time-dependent methods are restricted like their time-independent analogs to systems with no more than 2–3 spatial degrees of freedom, progress in treating multidimensional systems has to rely on approximate methods such as the time-dependent Hartree grid (TDHG) algorithm. This treatment is based on the enforced factorization of the time-dependent wavepacket for the whole system into a product of one-dimensional factors, one for each degree of freedom. Each of these is then evolved on a one-dimensional grid in its own (one-dimensional) "variationally optimized" effective potential.[4,5] In this framework, to solve a D-dimensional Schrödinger equation using numerical grids, using N points to span each dimension, requires ND points instead of the N^D points needed in an exact propagation scheme.

There are, nevertheless, processes for which TDH fails. This failure can be attributed to the "mean field" character of the propagation, which entails neglect of direct spatial correlation between degrees of freedom.[8] In previous papers,[9] we have shown how to produce exact wavepacket propagation using a configuration interaction scheme based on TDHG trajectories, and applied our method to some model cases. However, in order to demonstrate real utility, this extension of TDHG, which we have termed TDHG–CI, should be tested on systems with more than 2 degrees of freedom. It is the purpose of this paper to show how TDHG–CI performs in certain cases where propagation via standard grid-based exact wavepacket algorithms as well as time-independent methods is currently not feasible.

To this end, we study the photodesorption of a rigid rotor from a static solid surface. The desorption is induced by an ultraviolet (UV) photon that promotes the surface-adsorbate complex to a repulsive electronically excited surface. In this case, relevant experimental observables are the total photodissociation cross section and final rotational distributions.

In Sec. II we review the basic TDHG–CI equations of motion and introduce the potential energy function via which the diatom interacts with the corrugated solid surface in both ground and excited electronic states. Then in Sec. III, we present results for several parameter sets. The convergence of our CI results is demonstrated, and comparison to TDHG results is made. The paper concludes with a Discussion Section, IV, where our main results are summarized, and avenues for further research are sketched.

II. THEORETICAL BACKGROUND

A. Basic TDHG and CI equations

Consider a rigid rotor with masses M_A, M_B, and (fixed) bond length r, adsorbed on a static surface. The system is completely specified by the coordinates of the center of mass of the diatom $\mathbf{R}=(x,y,z)$ and the polar angle θ and azimuthal angle ϕ of the relative coordinate

[a]Permanent address: Instituto de Matemáticas y Física Fundamental (C.S.I.C), Calle Serrano 123, E-28006-Madrid Spain.
[b]Camille and Henry Dreyfus Teacher-Scholar.

vector (pointing fom M_A to M_B) with respect to the surface. Then, the total Hamiltonian for motion on a given Born–Oppenheimer potential surface $V(\mathbf{R},\theta,\phi)$ can be written as

$$H(\mathbf{R},\theta,\phi)=-\frac{\hbar^2}{2M}\nabla_R^2+\frac{\hat{L}^2}{2\mu r^2}+V(\mathbf{R},\theta,\phi), \tag{1}$$

where $M=M_A+M_B$ is the total mass, $\mu=M_AM_B/(M_A+M_B)$ is the reduced mass of the diatom, ∇_R^2 is the Laplacian operator associated with the center of mass vector, and $\hat{L}^2$ is the usual squared angular momentum operator (which depends upon the angular variables θ, ϕ).

There are many mechanisms via which photodesorption of molecules from solid surfaces can occur. Here, we consider the simplest case, dynamically, in which the photodesorption of the adsorbate–surface complex is achieved by UV photon induced excitation: the complex makes a direct transition from its ground electronic state to an excited electronic state that is purely repulsive along one or more coordinates. The standard prescription for studying the details of the frequency spectrum associated with this event requires the evolution of the ground state eigenfunction for the rovibrational nuclear motion $\Psi_g(\mathbf{R},\theta,\phi)$ on the excited potential energy surface.

Once this propagation has been carried out, the total absorption cross associated with continuous wave laser excitation at frequency ω_L is given by[10]

$$\sigma(\omega_L)=\frac{Re}{\pi}\int_0^\infty dt\exp\left(\frac{i}{\hbar}(\omega_L+E_g)t\right)\times\langle\Psi_g(\mathbf{R},\theta,\phi)\,|\,\Psi(\mathbf{R},\theta,\phi,t)\rangle, \tag{2}$$

where E_g is the energy eigenvalue corresponding to rovibrational eigenfunction $\Psi_g(\mathbf{R},\theta,\phi)$ and ω_L is the laser frequency. Finally, $\Psi(\mathbf{R},\theta,\phi,t)$ is the initial wavepacket propagated according to the Hamiltonian, Eq. (1), with $V(\mathbf{R},\theta,\phi)$ the potential surface associated with the excited elecronic state where the fragmentation takes place.

Notice that, strictly speaking, the above equation gives photodissociation probability per unit time per unit electric field strength squared. For comparison with experiments it should be normalized by the incident photon flux, which leads to an extra factor ω_L. For electronic absorption, the effect of this extra term is small and hence for the purposes of this paper can be neglected.

Partial cross sections are calculated by the usual asymptotic projection[11,12] (again, neglecting a slowly varying factor of ω_L):

$$\frac{d\sigma^{(\ell m)}(\omega_L)}{d\Omega}=\lim_{\tau\to\infty}|\langle\mathbf{K}_R|\langle Y_{\ell m}|\Psi(\mathbf{R},\theta,\phi,\tau)\rangle|^2. \tag{3}$$

Here $\langle\mathbf{R}\,|\,\mathbf{K}_R\rangle$ is an energy normalized outgoing plane wave corresponding to the center of mass momentum $\mathbf{K}_R$, and the $Y_{\ell m}$ are normalized eigenstates of the free rotor (i.e., spherical harmonics). This quantity is a function of the wave vector $\mathbf{K}_R$, or equivalently its translational energy at given polar angle θ and azimuthal angle ϕ. The integration of these differential partial cross sections over all solid angles yields the partial cross section (PCS) for dissociation into diatomic rotational state (ℓm) at a given incident laser frequency ω_L, that is

$$\sigma^{(\ell m)}(\omega_L)=\int_0^{2\pi}d\phi\int_0^\pi d\theta\sin\theta\frac{d\sigma^{(lm)}(\omega_L)}{d\Omega}.$$

Finally, when we add up the contributions of all final rotational states, we will get the total cross section (TCS): $\sigma(\omega_L)=\Sigma_{\ell m}\sigma^{(\ell m)}(\omega_L)$. Cross sections obtained by this procedure must be equal to those extracted from Eq. (2) if the wavepacket $\Psi(\mathbf{R},\theta,\phi,t)$ is propagated exactly for all times.

Note that a TCS spectrum completely equivalent to the one obtained by summing all partial cross sections can be procured by Fourier transforming the "long-time correlation function" $\langle\Psi(\mathbf{R},\theta,\phi,\tau)\,|\,\Psi(\mathbf{R},\theta,\phi,\tau+t)\rangle$ in a manner analogous to the transformation of the "short-time correlation function" indicated in Eq. (2). This "long time correlation function" provides a useful check on the complete and accurate enumeration of individual partial cross sections.

For the initial ground state, we have utilized a Cartesian wavepacket to describe the motion of the diatomic center of mass, whereas its orientation has been described through a time-dependent superposition of spherical harmonics.[13] More precisely, our TDHG trial wavepacket is

$$\Psi(\mathbf{R},\theta,\phi,t)=\phi_x(x,t)\phi_y(y,t)\phi_z(z,t)\Theta(\theta,\phi,t)\times\exp\left(\frac{iS(t)}{\hbar}\right), \tag{4}$$

with $S(t)$ a phase factor isolated in order to simplify the equations of motion. Its explicit form for this case, as obtained from the McLachlan variational principle,[4] is $S(t)=\int_0^t dt'\,v(t')$, with

$$v(t)=3\int|\phi_x\phi_y\phi_z\Theta|^2V(x,y,z,\theta,\phi)\,dx\,dy\,dz\sin\theta\,d\theta\,d\phi. \tag{5}$$

[The TDH equations of motion that govern the evolution of each of the factors are discussed below. Notice that the (θ,ϕ) motion is treated via one wavepacket. This is due to the strong intrinsic coupling between these coordinates; again, cf. below. The TDH approximation is very flexible as regards the way in which degrees of freedom are partitioned.]

The initial wavepacket is based on a scenario in which the diatomic molecule librates prior to electronic excitation around an orientation normal to the solid surface ($\theta=0$). It is further assumed, for simplicity, that the vibration of the diatom's center of mass about its equilibrium position above the surface is substantially higher in frequency than is the libration of the diatom's relative coordinate vector about the normal to the surface. Based on these assumptions we write the initial wavepacket as a product of one-dimensional Gaussians for each center of mass coordinate, and an angular function which reflects the librational characteristics of the angular motion on the ground state potential surface. To be more specific, $\Theta(\theta,\phi,0)$ is chosen to

be Gaussian-like in θ (peaked about $\theta=0$); the associated probability density might be envisaged as a polar icecap on the unit sphere. The factorized wavepacket just described constitutes the "ground state" or "guiding" wavepacket of the traveling basis set that will be utilized to perform CI corrections to the TDH level dynamics. It is convenient to construct a basis set "on top of" the initial guiding wavepacket, since our CI algorithm guarantees that an initially orthonormal basis will remain orthonormal, and this feature greatly simplifies the CI equations of motion. It is easy to build an orthonormal "harmonic oscillator" type "excited" basis function on top of the Cartesian Gaussian wavepackets associated with each of the three center of mass coordinates.[9a,14]

For the angular degrees of freedom θ and ϕ this task is a little subtler. We are dealing with a rigid rotor exhibiting restricted motion around $\theta=0$, i.e., a hindered rotor. Hence, we assume that on the ground electronic potential surface the angular motion is described by the standard hindered rotor potential[15] $V_0(1-\cos\theta)$. For small oscillations this potential reduces to a $V_0\theta^2/2$ harmonic oscillator type potential. The ground state eigenfunction of the (full) hindered rotor potential will therefore have the Gaussian-like shape described in the previous paragraph. (The reduction to harmonic oscillation in the small librational limit also provides a way to determine V_0 in terms of the experimentally measurable librational frequency of the hindered rotor, as discussed below in Sec. III.) To determine the ground state of the hindered rotor we expand the Hamiltonian

$$H_{\theta,\phi}=\hat{L}^2/2\mu r^2+V_0(1-\cos\theta)$$

in a basis of spherical harmonics. In addition to the ground state angular eigenfunction, in which we assume the system to be prepared and which is used as the "guiding wavepacket" in our TDHG–CI procedure, this calculation produces a naturally orthogonal set of excited eigenstates of the hindered rotor Hamiltonian which can be used as the initial "excited" basis packets in our expansion of the exact wavepacket for the overall system [cf. Eq. (6) below]. [Of course, the ground state, having azimuthal symmetry, will be a linear combination of $m=0$ spherical harmonics only. Because of the nature of the excited state potentials assumed in this work (cf. Sec. II B below), only basis wavepackets with azimuthal symmetry will be required. Hence the expansion of the librational eigenfunctions in spherical harmonics can be restricted to an expansion in Legendre polynomials.]

Once we have an appropriate set of "excited states" (basis functions) for each degree of freedom, we then consider a superposition of basis functions of the type given by Eq. (4), i.e., we have the following total wavepacket:

$$\Psi(\mathbf{R},\theta,\phi,t)=\sum_{ijkl} a_{ijkl}(t)\omega_{ijkl}(\mathbf{R},\theta,\phi,t). \tag{6}$$

Here

$$\omega_{ijkl}(\mathbf{R},\theta,\phi,t)=\phi_x^i(x,t)\phi_y^j(y,t)\phi_z^k(z,t)\Theta^l(\theta,\phi,t)\times\exp\left(\frac{iS(t)}{\hbar}\right),$$

and the sum is taken independently over indices i,j,k,l to generate a direct product basis set. (The index l labels the angular basis functions, which are, in general, functions of the angles θ and ϕ. It should not be confused with the total angular momentum index ℓ that appears in the spherical harmonic functions used to construct the angular basis functions.) In the limit that these indices have infinite range, the expansion becomes complete. In practice, we truncate the basis at a finite upper limit, and increase this limit until convergence of the wavepacket dynamics is achieved. By choosing all $a_{ijkl}(0)=0$, except one, say $a_{i'j'k'l'}(0)=1$, we select our wavepacket at time $t=0$. The relevant values of $(i'j'k'l')$ needed to make the wavepacket at $t=0$ be equal to $\Omega_g(\mathbf{R},\theta,\phi)$ are obvious for the examples presented below (cf. Sec. III).

Now, as has been extensively discussed in Ref. 9(a), *all* the wavepackets associated with a particular coordinate are propagated under *the same effective potential.* Hence, the equations of motion become:

$$i\hbar\frac{\partial\phi_x^i}{\partial t}=-\frac{\hbar^2}{2M}\frac{\partial^2\phi_x^i}{\partial x^2}+\langle\bar{\phi}_y\bar{\phi}_z\bar{\Theta}|\,V(x,y,z,\theta,\phi)\,|\bar{\phi}_y\bar{\phi}_z\bar{\Theta}\rangle\phi_x^i \tag{7}$$

and analogously for y and z. Because of the nonseparable character of the $\hat{L}^2$ operator, the angular variables are treated together, in accord with the following equation:

$$i\hbar\frac{\partial\Theta^l}{\partial t}=\frac{\hat{L}^2}{2\mu r^2}\Theta^l+\langle\bar{\phi}_x\bar{\phi}_y\bar{\phi}_z|\,V(x,y,z,\theta,\phi)\,|\bar{\phi}_x\bar{\phi}_y\bar{\phi}_z\rangle\Theta^l. \tag{8}$$

Here, $\bar{\phi}_x,\bar{\phi}_y,\bar{\phi}_z,\bar{\Theta}$ are the "guiding" packets which determine the effective potentials that appear in Eqs. (7),(8), and the phase factor $S(t)$. In this work, guiding packets evolve out of Ψ_g [the basis packet $(i'j'k'l')$ discussed above]. The TDH equations of motion utilized for this purpose are essentially Eqs. (7) and (8) with the mean field potentials determined self-consistently in the course of the evolution. See Ref. 12 for details.

In order to solve Eq. (8) numerically, the angular wavepackets, expanded in terms of spherical harmonics, $\Theta^i(\theta,\phi,t)=\Sigma_{\ell m}b^i_{\ell m}(t)Y_{\ell m}(\theta,\phi)$, are substituted into Eq. (8), yielding a set of first-order differential equations that governs the evolution of the angular part.[12,13] An alternative way to proceed would be to use a grid expansion over the unit sphere and track the angular basis functions via discretization on this grid.[16] This alternate route may prove advantageous for situations (such as those considered here) where there is extensive rotational excitation, and hence a large basis of spherical harmonics is required in the time-dependent expansion procedure just described.

Now, when the trial wave function, Eq. (6), is substituted into the full time-dependent Schrödinger equation, $i\hbar\,\partial_t\Psi=H\Psi$, with H given by Eq. (1), we get evolution equations for the coefficients $a_{ijkl}(t)$:

TABLE I. Potential parameters for parameter set I.

D (eV)	α (Å^{-1})	β_1	β_2	a (Å)	γ
0.167	5.0	0.05	0.75	2.01	1.0

TABLE II. Potential parameters for parameter set II.

D (eV)	α (Å^{-1})	β_1	β_2	a (Å)	γ
0.167	7.0	0.05	0.05	2.01	0.8

$$i\hbar\dot{a}_{ijkl}(t)=\sum_{i'j'k'l'}H_{ijkl,i'j'k'l'}a_{i'j'k'l'}(t), \tag{9}$$

where the time-dependent matrix elements are computed according to

$$H_{i'j'k'l',ijkl}=\langle\phi_x^{i'}\phi_y^{j'}\phi_z^{k'}\Theta^{l'}|\Delta V|\phi_x^{i}\phi_y^{j}\phi_z^{k}\Theta^{l}\rangle, \tag{10}$$

with

$$\Delta V=V(\mathbf{R},\theta,\phi)-[\langle V\rangle_{xyz}+\langle V\rangle_{xy\theta\phi}+\langle V\rangle_{xz\theta\phi}+\langle V\rangle_{yz\theta\phi}-v(t)]. \tag{11}$$

The notation $\langle V\rangle_{\alpha\beta\gamma\delta}$ indicates an average of the interaction potential over the probability density associated with the guiding wavepackets in the subscripted variables.

B. The potential

For the numerical work to be presented in Sec. III, we have taken a heteronuclear diatomic with masses of 12 and 16 amu, and a bond length of 1.1 Å. The potential mimics the interaction of a CO rotor with a rigid LiF crystal on its (100) face, and for the excited electronic state has the functional form:

$$V(\mathbf{R},\theta,\phi)=V_1(\theta,\phi)V_2(\mathbf{R}), \tag{12}$$

with

$$V_1(\theta,\phi)=1+\gamma P_2(\cos\theta),$$
$$V_2(\mathbf{R})=De^{-\alpha z}\{1-2[\beta_1\cos(\epsilon x)+\beta_2\cos(\epsilon y)]\}, \tag{13}$$

and $\epsilon=2\pi/a$, where a is the lattice spacing. This type of potential has been widely used in gas surface scattering studies[17] and more recently in the context of UV photodesorption of molecules from surfaces at finite temperatures.[12] It pertains to the case where the diatomic is oriented perpendicular to the surface with the 12 amu mass pointing in. Note that the excited state potential we have adopted is independent of azimuthal angle ϕ. The initial ground state motion, in which the molecule librates about polar angle $\theta=0$, corresponds to an initial wavepacket which is also ϕ independent. These two features enable us to significantly simplify our description of the angular motion on both the ground and excited potential surfaces. In particular, all relevant angular basis functions can be expanded in terms of $m=0$ spherical harmonics, i.e., Legendre polynomials in the polar angle θ. The dependence of the dynamics on azimuthal angle ϕ is thus completely removed, without loss of generality.

III. RESULTS

In order to demonstrate the utility of our algorithm we have carried out calculations on the system described above for several sets of potential parameters. Representative results are presented in this section for the two parameter sets listed in Tables I and II. All computations were based on the same ground state potential surface, assumed harmonic, and corresponding to an angular frequency $\omega_R=500\ \text{cm}^{-1}$ in each of the diatom center of mass degrees of freedom. For the polar angle coordinate (which represents libration about the "polar icecap") the ground state has been taken such that the "harmonic approximation" yields $\omega_\theta=100\ \text{cm}^{-1}$, where $\omega_\theta=(V_0/\mu r^2)^{1/2}$.

For direct photodesorption on a single electronically excited potential surface, the TDHG method often works quite well. This was found to be the case in Ref. 12, and consequently we have modified the potential parameters used in that work to "force" stronger interdimensional coupling. To further test the TDHG–CI algorithm, we have focused on the case that the initial wavepacket is vibrationally excited. We know from previous work that the time-dependent Hartree approximation is strained in propagating spatially extended wavepackets associated with excited vibrational states.[8] The necessity of computing spectra corresponding to vibrationally excited initial states that arise, for example, in finite temperature processes, provides further motivation for this choice.

For the parameter set I, listed in Table I, there is strong coupling between the dissociative coordinate z and the angular coordinate θ, as reflected in the value of the parameter $\gamma=1.0$, and with the y coordinate ($\beta_2=0.75$). The initial wavepacket considered was $\Psi(\mathbf{R},\theta,\phi)=\phi_x^0(x)\phi_y^0(y)\phi_z^2(z)\Theta^1(\theta)$. Note the excited vibrational motion along the z component of the center of mass and the libration of the diatom about the perpendicular to the surface. In Fig. 1 we show the total absorption cross section computed from short time wavepacket dynamics in

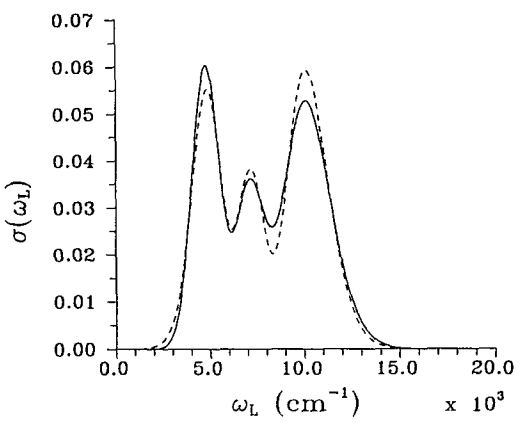

FIG. 1. Total cross section with the parameters in Table I and initial conditions discussed in text. Solid line is the result for the TDHG–CI, while the dashed line represents a calculation with a single TDHG trajectory.

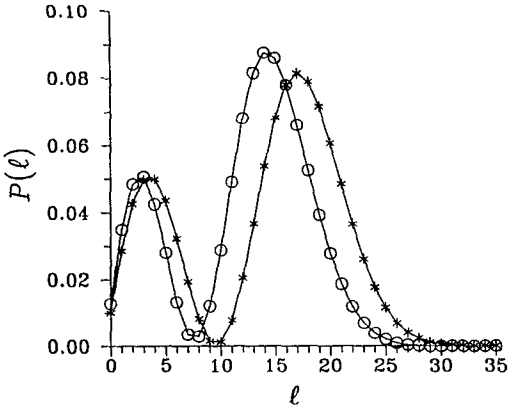

FIG. 2. Rotational excitation measure $P(\ell)$ defined in text. Circles (TDHG–CI), stars (TDHG). The calculation corresponds to the parameters in Table I and initial conditions discussed in text.

the Franck–Condon region. Comparison is made between results extracted from TDHG wavepacket propagation (dashed line) and full TDHG–CI results (solid line). (Details of basis size, etc., are given below.) The two curves are qualitatively similar, although not in complete quantitative accord. This situation is not surprising, since the TDHG result cannot go too far wrong in the short time period involved. We expect that if TDHG dynamics develops defects, it will do so at longer rather than shorter times. Hence the "acid test" entails examining the asymptotic, post-desorption dynamics.

An indication that the details of the long time dynamics may elude the TDHG approximation in this case is obtained by looking at the degree of rotational excitation exhibited in the asymptotic wavepacket. A measure of this property is provided by the square moduli of the coefficients in the Legendre polynomial expansion of the asymptotic angular wavepacket, summed over all "basis" contributions [with each contribution weighted by $a_{ijkl}|^2$ to account for the probability to find the system in basis state $(ijkl)$]. This quantity shall be denoted as $P(\ell)$. It is shown in Fig. 2 for parameter set I. Considerable discrepancy between TDHG with versus without CI is apparent: rotational excitation is noticeably suppressed in an average sense when CI is performed.

The most highly resolved state to state information that can be obtained from a photodissociation experiment is the fragment distribution at a particular incident laser frequency, i.e., the partial photodissociation cross section. PCS computations are expected to be sensitive to approximations made in the wavepacket propagation, since they reflect the detailed shape of the wavepacket at long, post-dissociation times. Indeed, extraction of various PCS's according to Eq. (3) revealed large discrepancies between TDHG and TDHG–CI predictions. An example for the system studied in Figs. 1 and 2 is shown in Fig. 3, where results for angular momentum states $\ell=7,8$ are shown. The CI corrected results are thought to be nearly converged (as discussed below), and hence the need for CI in this particular calculation is demonstrated.

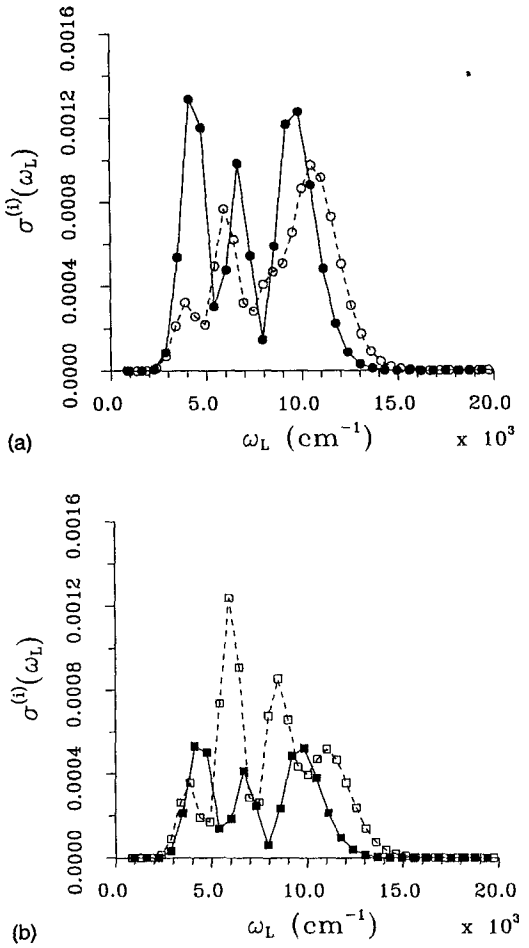

FIG. 3. Partial cross sections for Table I parameters and initial conditions discussed in text. Panel (a) depicts results for $\ell=7$: solid circles show TDHG–CI cross sections, open circles show TDHG cross sections. Panel (b) depicts results for $\ell=8$: solid squares show TDHG–CI cross sections, open squares show TDHG cross sections.

Analogous computations carried out with the potential parameters indicated in Table II showed similar features. As an example, we present results for the initial ground state wavepacket $\Psi_g(\mathbf{R},\theta,\phi)=\phi_x^0(x)\phi_y^1(y)\phi_z^3(z)\Theta^1(\theta)$. (Note the high degree of vibrational excitation in the cen-

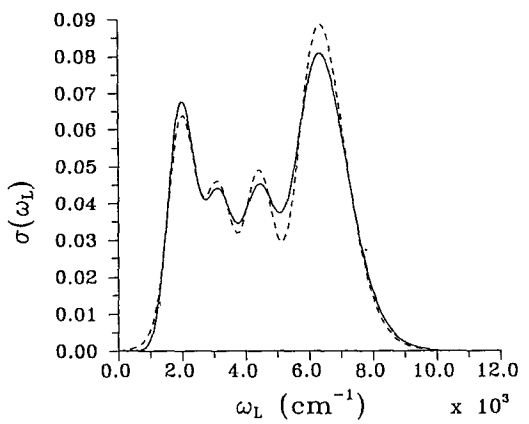

FIG. 4. Same as in Fig. 1 but for Table II and initial conditions discussed in text.

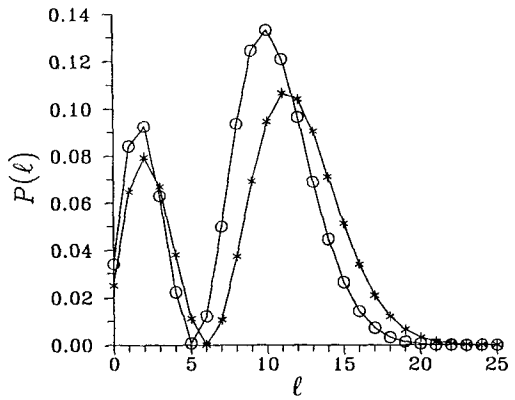

FIG. 5. Same as in Fig. 2 but for Table II and initial conditions discussed in text.

ter of mass motion.) Figures 4–6 contain, respectively, results for the total absorption cross section [obtained from short-time wavepacket dynamics via Eq. (2)], the rotational excitation measure $P(\ell)$, and the rotationally resolved partial desorption cross sections as a function of incident laser frequency for final rotational states $\ell = 18,19$. We see from Fig. 6 that the resolved partial cross sections computed within the TDHG approximation are again in substantial disagreement with their CI-corrected counterparts. The errors in individual PCS's are much more pronounced than the error in the TCS, which appears from Fig. 4 to be in reasonable agreement with the TDHG–CI result. The intermediate figure, Fig. 5, provides another measure of the errors accrued in TDHG dynamics at long times.

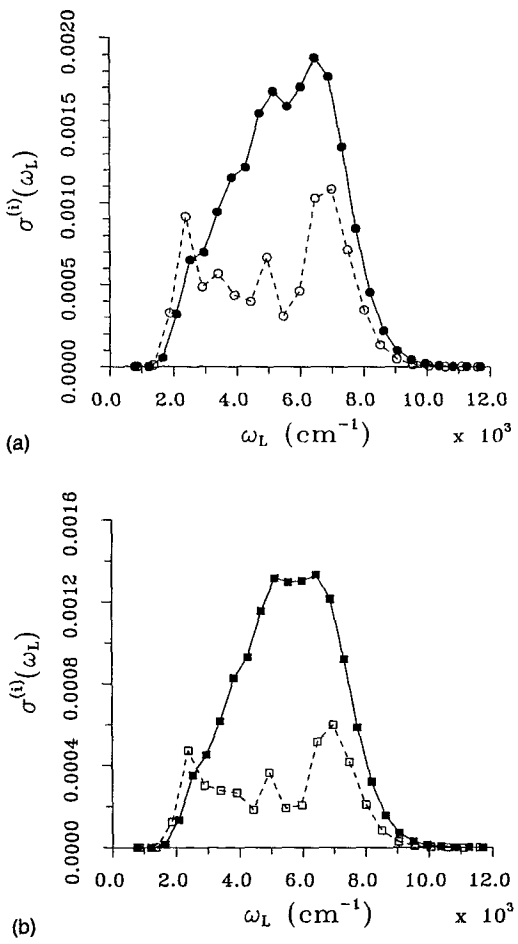

FIG. 6. Partial cross sections for Table II parameters and initial conditions discussed in text. Panel (a) depicts results for $\ell = 18$: solid circles show TDHG–CI cross sections, open circles show TDHG cross sections. Panel (b) depicts results for $\ell = 19$: solid squares show TDHG–CI cross sections, open squares show TDHG cross sections.

What is the confidence level in our CI results? The ultimate indicator is convergence of the basis expansion. In the systems under study here the strongest coupling occurs between z and θ coordinates. For the Table I results presented in Figs. 1–3, we used nine basis functions in z and eight in θ, while for the Table II results presented in Figs. 4–6, ten z basis functions and seven θ functions were used. The motion in x and y was found to be largely decoupled from the $z-\theta$ motion in the sense that the minimum basis set description of those coordinates sufficed. More precisely, for the Table I case, the minimum $x-y$ basis set consisted of the Gaussian guiding wavepackets. In the Table II case, the first excited state in the y direction is included in the minimum basis set. We found that when the $x-y$ basis expansion was "padded" with one extra function in each direction, (i.e., for the Table I case first excited states in x and y were added, and for the Table II case the first excited state in x and the second excited state in y were added), the coefficients of all "padded" basis functions in the complete 4-d basis set never grew beyond 10^{-10} in magnitude. Adding a second padding function had the same negligible effect.

To further check the accuracy of the CI corrections we compared the sum of all partial cross sections with the total cross section obtained via short-time wavepacket dynamics. The sum over partial cross sections was carried out by brute force, and checked by the "long-time" correlation function procedure discussed in Sec. II A. Essentially the same spectrum was obtained via both procedures.[18] Of course, if the wavepacket dynamics from which these cross sections are computed is exact for all times, then the total cross sections obtained by the two methods must be identical. However, any errors in the evolving wavepacket trajectory can lead to discrepancies between the two predictions. The comparison between short and long time TCS's is shown in Fig. 7 for the Table I system and Fig. 8 for the Table II system. The first of each pair shows TDHG–CI results and the second shows results for TDHG without CI corrections. It is clear for both parameter sets that the CI-corrected partial cross sections sum to a total cross section that is noticeably more consistent with the short-time version than the PCS's obtained from uncorrected TDHG dynamics. This provides further evidence of the accuracy of the CI computations.

IV. DISCUSSION

We have applied our TDHG–CI wavepacket dynamics algorithm to a problem involving four coupled spatial de-

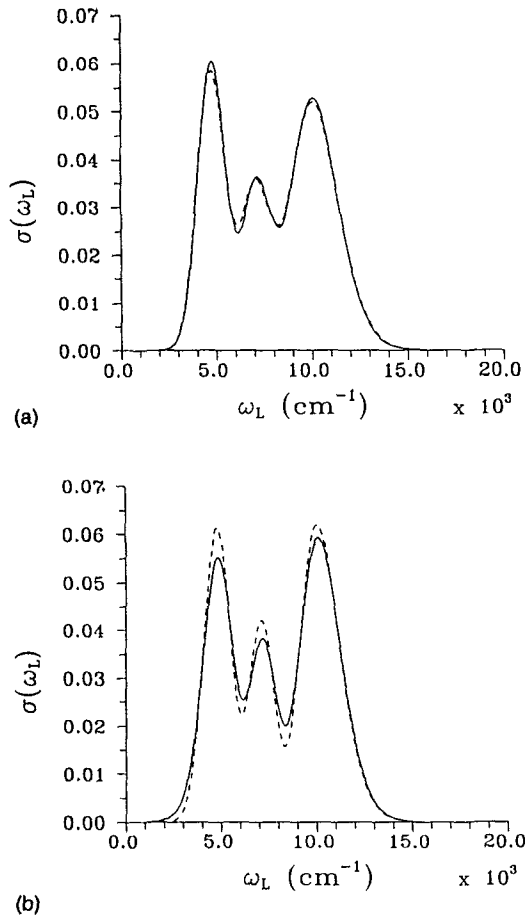

FIG. 7. (a) Comparison of TCS for short-time (solid lines) and long-time dynamics (dashed line) when TDHG–CI is used. (b) Same as (a) but using TDHG. Results are for parameters in Table I and initial conditions discussed in text.

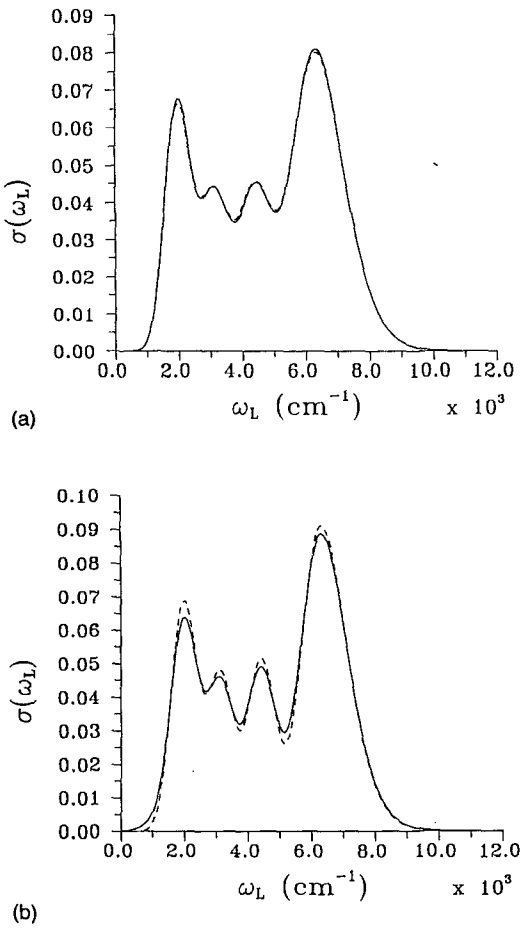

FIG. 8. (a) Comparison of TCS for short-time (solid lines) and long-time dynamics (dashed line) when TDHG–CI is used. (b) Same as (a) but using TDHG. Results are for parameters in Table II and initial conditions discussed in text.

grees of freedom, namely the photodesorption of a diatomic molecule from a corrugated solid surface (in a model where the diatom bond is frozen and azimuthal dependence of the interaction potential is neglected). This system would be difficult to treat via traditional time-independent methodologies due to the lack of periodicity of the ground state potential along the solid surface.[17] However, it presents no particular problem to time-dependent methods that do not rely on channel expansions (e.g., in two-dimensional plane waves corresponding to motion parallel to the surface). We have checked for convergence of the CI corrections in two ways, namely (1) by padding the basis expansion with additional excited states and checking that these states, which are initially unpopulated, do not become populated during the course of the wavepacket trajectory, and (2) by comparing total absorption cross sections (TCS's) extracted from short and long time dynamics. As in previous work, we find here that uncorrected TDHG wavepacket dynamics can develop substantial errors when the initial state is a spatially extended excited vibrational/librational state. Thus, in cases where it is necessary to compute photodissociation cross sections of vibrationally excited molecules, for example, for systems prepared at finite temperature, inclusion of CI corrections appears to be essential to obtain accurate results.

There are, naturally, a number of schemes for building correlation corrections into an expansion in product time-dependent basis functions of TDH type. In our TDHG–CI scheme, a basis set of time-dependent wavepackets is constructed simply from a single "guiding" TDH type wavepacket trajectory. Evolution of the basis functions is easy, preservation of orthonormality between them is automatic, the equations of motion for the time evolution of the coefficients which prescribe the configuration interaction are elementary, and the computation of time-dependent matrix elements that drive the coefficient evolution is efficient. The disadvantage of the method is that the basis functions are predetermined: there is no feedback mechanism that would allow them to adjust to the CI coefficient evolution. Indeed the basis functions in our procedure are not even individually preoptimized, but rather are completely determined by the trajectory of a single guiding wavepacket. (Some progress in removing this restriction has been recently reported by Gerber and Alimi.[19])

A promising procedure in which all "single particle" basis functions are evolved in tandem along with the CI

coefficients has been developed by Manthe *et al.*[20] This method enables optimum tuning of the zeroth order basis set and eliminates the need to anticipate the evolution of the true wavepacket in any way. The disadvantage of this method is the complexity of the equations of motion, and the comparatively elaborate coupling between all single particle basis packets and CI coefficients that is entailed in the construction of the single particle evolution equations.

In this work we have shown that our simple TDHG–CI scheme works well for direct photodissociation dynamics, even on spatially extended initial states. In particular, several important features of the algorithm have been demonstrated for the first time. These include feasability in more than two spatial dimensions, and incorporation of internal motion described by non-Cartesian coordinates. One of the strengths of the algorithm, namely, the ability to focus effort on the most strongly coupled degrees of freedom, has also been illustrated. In the photodesorption events studied herein, two degrees of freedom were strongly coupled, while two others could be treated satisfactorily within the TDH approximation. The ability of the method to systematically check the adequacy of minimum basis representations in certain degrees of freedom is important. Due to the rapid growth in the number of product basis functions needed to span configuration space with spatial dimensionality, it will be essential to identify weakly correlated degrees of freedom that can be treated within the TDH approximation if the quantum dynamics of polyatomic molecules and condensed phase systems is to be treated accurately.

ACKNOWLEDGMENTS

This work was partially supported by EEC Grant No. SC1.145.C. RDC acknowledges financial support from the National Science Foundation, Grant No. CHE-9101432, and the Camille and Henry Dreyfus Foundation. We would also like to thank D. G. Evans for help with the computation of the rigid rotor librational eigenfunctions. Many of the computations were carried out at the Pittsburgh Supercomputer Center.

[1] For a review of recent work in the field, see, for example, Comp. Phys. Rep. **63**, (1991).
[2] R. Kosloff, J. Phys. Chem. **92**, 2087 (1988).
[3] Recent reviews, particularly in the context of molecule-surface interactions, include: (a) R. B. Gerber, R. Kosloff, and M. Berman, Comp. Phys. Rep. **5**, 59 (1986); (b) G. D. Billing, Comp. Phys. Rep. **12**, 384 (1990).
[4] A. D. McLachlan, Mol. Phys. **8**, 39 (1964).
[5] R. Alimi, R. B. Gerber, A. D. Hammerich, R. Kosloff, and M. A. Ratner, J. Chem. Phys. **93**, 6484 (1990); M. Messina and R. D. Coalson, J. Chem. Phys. **90**, 4015 (1989).
[6] R. B. Gerber, Chem. Rev. **87**, 29 (1987).
[7] A. E. DePristo and A. Kara, Adv. Chem. Phys. **77**, 163 (1989).
[8] R. D. Coalson, Chem. Phys. Lett. **90**, 443 (1990).
[9] (a) J. Campos-Martínez and R. D. Coalson, J. Chem. Phys. **93**, 4740 (1990); (b) J. Campos-Martínez, J. R. Waldeck, and R. D. Coalson, J. Chem. Phys. **96**, 3613 (1992).
[10] (a) M. Lax, J. Chem. Phys. **20**, 1752 (1952); (b) E. J. Heller, J. Chem. Phys. **68**, 3891 (1978).
[11] (a) K. C. Kulander and E. J. Heller, J. Chem. Phys. **69**, 2439 (1978); (b) S. Y. Lee and E. J. Heller, J. Chem. Phys. **76**, 3035 (1982).
[12] (a) M. Messina and R. D. Coalson, J. Chem. Phys. **95**, 5364 (1991); (b) M. Messina and R. D. Coalson, J. Chem. Phys. **95**, 8977 (1991).
[13] B. Jackson and H. Metiu, J. Chem. Phys. **84**, 3535 (1986).
[14] R. D. Coalson and M. Karplus, Chem. Phys. Lett. **90**, 301 (1982).
[15] (a) G. Herzberg, *Molecular Spectra and Molecular Structure* (Van Nostrand Reinhold, New York, 1945), (b) L. Pauling, Phys. Rev. **36**, 430 (1930).
[16] C. E. Dateo and H. Metiu, J. Chem. Phys. **95**, 7392 (1991).
[17] G. Wolken, Jr., J. Chem. Phys. **58**, 3047 (1973).
[18] Small differences were observed in the explicit "sum over partials" versus the "long-time correlation function" results. These were attributed primarily to precision error accumulated in computing all the partial cross sections via projection onto asymptotic fragment states. Since the discrepancies are quite minor, only the "long-time correlation function" results are displayed.
[19] R. B. Gerber and R. Alimi, Chem. Phys. Lett. **184**, 69 (1991).
[20] (a) J. Kucar, H.-D. Meyer and L. S. Ceberdaum, Chem. Phys. Lett. **140**, 525 (1987); (b) H.-D. Meyer, J. Kucar, and L. S. Cederbaum, J. Math. Phys. **29**, 1417 (1988); (c) U. Manthe, H.-D. Meyer, and L. S. Cederbaum, J. Chem. Phys. **97**, 9062 (1992).